



Prediction of scattering effects by sonic crystal noise barriers in 2d and 3d finite difference simulations

Sorrel Hoare, Damian Murphy

► To cite this version:

Sorrel Hoare, Damian Murphy. Prediction of scattering effects by sonic crystal noise barriers in 2d and 3d finite difference simulations. Acoustics 2012, Apr 2012, Nantes, France. ⟨hal-00810977⟩

HAL Id: hal-00810977

<https://hal.science/hal-00810977v1>

Submitted on 23 Apr 2012

HAL is a multi-disciplinary open access archive for the deposit and dissemination of scientific research documents, whether they are published or not. The documents may come from teaching and research institutions in France or abroad, or from public or private research centers.

L'archive ouverte pluridisciplinaire **HAL**, est destinée au dépôt et à la diffusion de documents scientifiques de niveau recherche, publiés ou non, émanant des établissements d'enseignement et de recherche français ou étrangers, des laboratoires publics ou privés.



HAL Authorization



ACOUSTICS 2012

Prediction of scattering effects by sonic crystal noise barriers in 2d and 3d finite difference simulations

S. H. Hoare and D. T. Murphy

Department of Electronics [York], Department of Electronics, The University of York,
Heslington Lane, YO105DD York, UK
shnh500@ohm.york.ac.uk

Sonic crystals have been investigated in recent years both as a potential form of noise barrier, and as a form of sonic art aimed at enhancing perception of the surrounding acoustic environment. The broader aim of this research is concerned with the auralization of these structures, which has, as yet, rarely been attempted. In a previous publication, prediction of the acoustic wave propagation through 2-D arrays of solid, cylindrical scatterers embedded in air was performed in 2-D Finite Difference Time Domain (FDTD) simulations. In this paper, the model has been extended into the third dimension and the results are compared with those obtained in the previous experiment. In both the 2-D and 3-D simulations the location of the fundamental band gap corresponds with the predicted location - predictions being based on simple theoretical considerations relating the frequency of the transmission gaps to the array configuration.

1 Introduction

In 1995 the artist Eusebio Sempere created a sculpture composed of a three-dimensional array of polished stainless-steel tubes with a rotating base. As well as being visually arresting, it was also observed that the sculpture behaved as a sonic filter that blocked transmission of particular frequencies. A listener on one side heard a tonal modification of those sound sources located on the other side, the visual equivalent of coloured glass prisms [1]. The sculpture captured the interest of several scientists who anticipated the application of such structures in environmental noise control. Meseguer et al. posited that, in addition to blocking sound, the structures might even be used to transform unpleasant environmental noise into something far more soothing [2]. The use of sonic crystals as a form of noise barrier has been the subject of investigation in recent years, notably in the work of Sanchez-Perez et al. [3].

Sonic crystals have also attracted interest from other artists as well as scientists. In 2009 Sound consultancy Liminal designed a structure intended to 'recycle' the sounds of the city, turning unwanted environmental noise into sound with a more 'musical' quality. Their work, entitled 'The Organ of Corti' is a portable device to be placed near to a source of white noise, such as a motorway or river wharf. Depending on the nature of the sound source and the position of the listener, it was posited that interesting filtering effects would be audible [4]. Based on comments posted on internet forums such as wired.co.uk [5], it would seem that whilst the concept was generally well-received, the success of the structure as a sound augmenting device was perhaps limited. It is possible that more complex structures could produce a more remarkable effect. It is thought here that the use of auralization as a design tool might aid the development of such structures.

As yet there has been little attempt to auralise sonic crystals during the planning process. It is our belief that this could help in several ways. Firstly, it would allow the designer to fine-tune the design from a listener's perspective; secondly, it would allow the designer to experiment more freely with designs of a higher complexity; and thirdly, it may help to optimise the design for a particular space - perhaps one known to suffer from the adverse effects of environmental noise. It is hoped that sufficiently 'true-to-life' auralizations may assist in securing the future of sonic crystals as interesting and acoustically beneficial ornaments in noisy environments. The wider aim is therefore to develop a robust method for simulating the impulse response (IR) at observation points located on the opposing side of a sonic crystal barrier to a broadband noise source. auralizations may then be performed through convolution of environmental sound recordings with the synthetic IRs and, in conjunction with appropriate visualisation, a fairly realistic representation of

a sound environment would then be subjected to perceptual evaluation.

2 Background

When sound waves propagate within a crystalline structure, they are scattered through interaction with atoms or elements in the material. At certain frequencies and angles of incidence, either or both of the following scenarios may ensue: intense peaks of reflected radiation over a narrow range of frequencies; a pattern of standing waves signifying a band gap in the frequency spectrum of the transmitted signal. Considering the analogous phenomenon of electromagnetic waves, these effects may be observed in real crystals and explains the vivid colouration and iridescent appearance of some gemstones. W. L. Bragg explained the phenomena by considering the crystal as a set of discrete parallel planes separated by a constant parameter d (figs. 1 and 2). 'Bragg peaks' as the peaks came to be known, are said to be the result of constructive interference between reflections off the various planes, whilst band gaps are the result of destructive interference between the overlapping waves. Interference is constructive when the phase shift is a multiple of 2π and destructive at odd multiples of π ; a condition which can be expressed by Bragg's law,

$$2d \sin \theta = n\lambda \quad (1)$$

where n is an integer determining the reflection order, λ is the wavelength and θ is the scattering angle. With the substitution of the distance d for the lattice constant denoted a , the centre frequency of the band gap is thus given by,

$$f_c = \frac{c}{2a} \quad (2)$$

where c is the speed of sound in air. In theory a band gap will occur at multiples of the fundamental affected frequency, hence it is common to refer to multiple band gaps as a periodic band gap (PBG). The width of the band gap is determined by the filling fraction - i.e. the fraction of the structure occupied by the cylinders [6]. For a square lattice arrangement, the filling fraction, F , is given by,

$$F = \frac{\pi\phi^2}{4a^2} \quad (3)$$

where ϕ is the diameter of the cylinders and a is the lattice constant. Experiments performed in [6] and [7] suggest that a filling fraction of around 0.3-0.4 is optimum for a wider band gap.

In crystallography the dimensionality of the structure relates to the number of directions in which the structure has periodicity. For example, in the case of a basic cubic lattice,

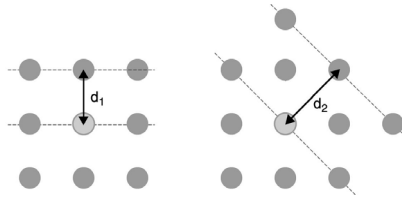


Figure 1: In the 2-D square lattice, waves are scattered from lattice planes, also known as Bragg planes, separated by the interplanar distance d . The first lattice plane lies between the primitive element and its nearest neighbours, the 2nd lies between its second-nearest set of neighbours, and so on.

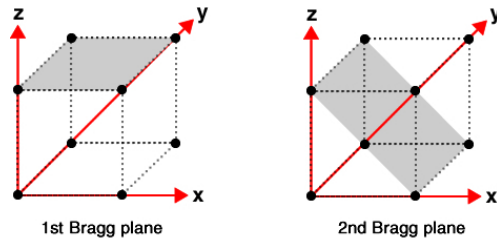


Figure 2: The first and second Bragg planes of a 3-D square lattice.

in 1-D the periodicity is in one direction only with the inclusions forming layers. In 2-D, the inclusions have infinite height but with periodicity in both the x and y directions. In 3-D, the structure is periodic in all 3 axial directions (fig. 3). In the cubic case, the limit is 3 dimensions, although higher dimensions are possible for different types of lattice.

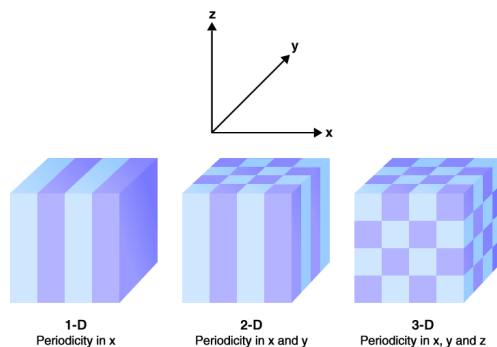


Figure 3: 1-D, 2-D and 3-D Periodic structures.

3 Method

The simulations presented here are of a 2-D sonic crystal with cylindrical steel rod-like inclusions. The layout of the simulation domain in 3-D and 2-D are depicted in figs. 4 and 5 respectively. Using (1) and taking the lattice constant to be 0.11m, it is thought the fundamental band gaps for the first and second Bragg planes are likely to occur around 1.6kHz and 1.1kHz, with secondary gaps occurring at multiples of these frequencies. According to (3), a cylinder radius of 3.5cm achieves a filling fraction of 0.32 which is within the optimum range. In reality, the existence of the PBG and its bandwidth are dependent upon more than the geometry of the array of inclusions. The material characteristics of the structure, specifically the contrast between its density and elastic properties, are also aspects for consideration. In previous 2-D simulations, it was found that varying the elastic properties

of the media did not have a substantial effect on the results of the simulations; hence, for greater efficiency, it has been assumed here that the surfaces of the inclusions are perfectly reflective and the velocity of sound may therefore remain a constant. Our method is therefore only applicable to structures composed of highly reflective materials as including their absorptive properties would require the reintroduction of the velocity component in the simulations.

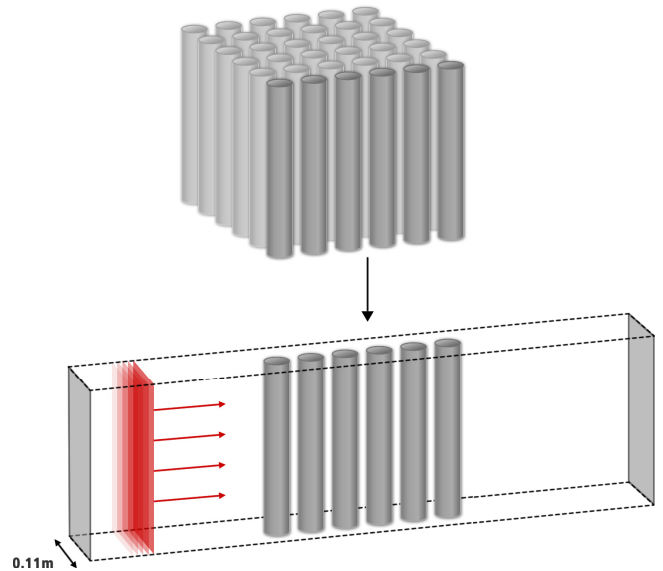


Figure 4: Layout of the 3-D simulation domain showing the portion of the structure to be simulated. Padding is applied at either end to eliminate reflections.

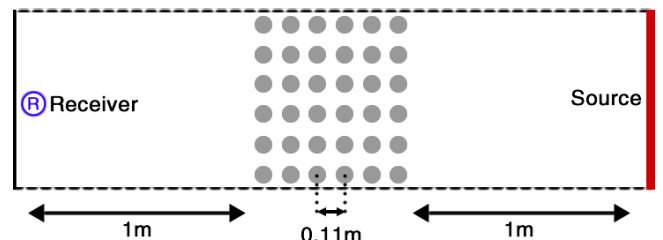


Figure 5: Layout of the 2-D simulation domain. Padding is applied at either end to eliminate reflections.

3.1 3-D Simulations

Due to the translational symmetry of the structure in two dimensions, it is not necessary to discretise and perform a simulation of the entire structure. To economise on speed of calculation and memory usage, only a thin segment of the 3-D structure is simulated (fig. 4), and at each of the 4 sides of the segment and their respective edges, a periodic boundary condition (PBC) is applied.

Translational symmetry describes the invariance of a system of equations under any translation. In crystallographic terms, the system equates to the primitive or unit cell of the crystal lattice - a structure comprised of identical parts arranged in a repeating pattern. A translation therefore represents a spatial 'shift' from a point in the unit cell, in a given direction and by a certain distance, a , referred to as the lattice constant, such that one arrives at the exact same point in a neighbouring cell.

$$T(x) = T(x + a) \quad (4)$$

It also implies that in each of the two dimensions having translational symmetry, the object is of infinite proportions. This precludes diffraction of sound around the top and sides of the barrier - an effect which is more pronounced at lower frequencies where wavelengths are long in relation to the barrier dimensions. Also excluded from the model are the effects of local resonance. At certain frequencies, the natural resonances of a real solid structure may be excited, causing the object to vibrate at an audible frequency. Should this happen, the structure has effectively become an acoustic source in its own right. Once again, this is an effect more often observed at lower frequencies. The main implication of all this is that the modelled impulse response is likely to lack the low frequency components that would be conspicuous in a real-world scenario as a result of diffraction and local resonance.

Using the 3-D standard leapfrog (SLF) compact explicit scheme described in [8], the implementation of the PBC is very simple. As we have seen, the requisite pressure components for performing the update equation are obtained from the neighbouring nodes. For nodes that lie on the boundary or an edge, the values of neighbouring nodes that would fall outside the simulation domain are simply replaced with those of their 'mirror images' (see fig. 6). For boundary nodes, only one pressure component needs substituting, whilst for edges and corner nodes, two and three pressure components are substituted respectively.

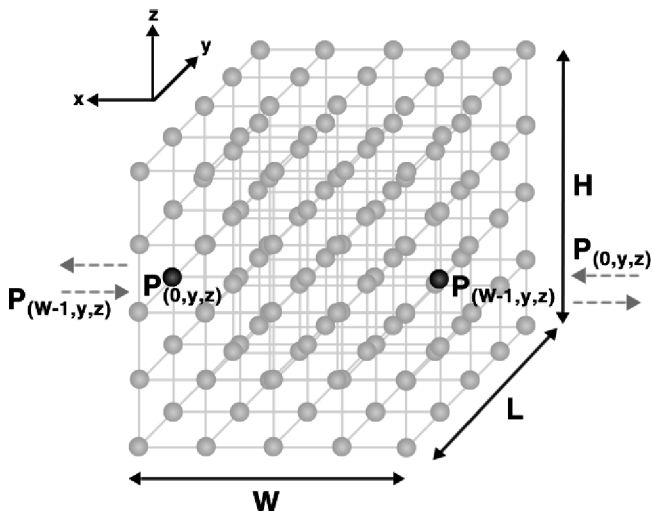


Figure 6: The 3-D rectilinear mesh. Pressure nodes where a PBC has been implemented derive their values from neighbouring nodes and 'mirror image' nodes.

The values of nodes at either end of the slice are held at zero; hence the ends behave as perfectly reflective boundaries. As one only wishes to capture the direct signal, it is therefore necessary to add sufficient space to the rear of the source and receiver so as to exclude the unwanted reflections from the impulse response. The simulation is performed for two different mesh resolutions, where the values of dx were given to be 5mm and 2.5mm. These equate to sampling rates of 118.67kHz and 237.34kHz respectively. It was found that values of dx above 5mm did not yield sufficient structural detail, while values below 2.5mm caused deterioration in the low frequency response due to shortening the duration of the IR in time.

A Gaussian source is implemented across a vertical cross-section of the mesh, stimulating a planar source. The planar nature of the source is significant as it implies that, given the periodicity of the crystal in 2 dimensions, the 2-D and 3-D simulations should yield identical results. Any slight differences would be a consequence of rounding error and some slight discrepancies in the sampling rate and window length. The purpose of doing the comparison is therefore to check that the 3-D model is in accordance with the 2-D model - vital if we are to progress onto modelling triply periodic structures as intended. There are, however, additional reasons why one might opt for a planar or line source in a situation such as this. Whereas a point source would yield a more general transform function of the structure, a planar source is more closely analogous to a near-field broadband noise source such as a road or a river, and as such, is more relevant to the intended application. Finally - and somewhat crucially - is the fact that the use of a point source here would prohibit the application of the PBC.

3.2 2-D Simulations

Previous simulations presented in [9] were performed using a point source and FDTD formulation in which velocity and pressure components were both modelled. In this paper, to enable a closer comparison between the 2-D and 3-D impulse responses, the 2-D SLF compact explicit scheme[10] has been used with a line source. The main benefit of this type of source is that it allows us to record IRs from any position on the rear face of the structure, whereas the point source prohibited measurements taken from anywhere other than a central point. As in the 3-D simulations, a PBC has also been applied to the left and right sides of the simulation domain. The perfect symmetry of the unit cell ensures that the results are identical for any number of columns. Once again, the simulations are performed twice for values of dx equal to 5mm and 2.5mm, both before and after the insertion of the sonic crystal, although this time the values of dx equate to sampling rates of 96.89kHz and 193.79kHz respectively. The difference can be explained by the fact that the temporal resolution of the mesh is limited by the Courant condition [11], which dictates

$$dt \leq \frac{dx}{\sqrt{d} \cdot c} \quad (5)$$

where dt is the time step, dx the cell size, c the speed of sound and d the number of dimensions.

3.3 Results

In figs. 7 - 10, the visualisations have been truncated to show only the region of interest. The source is travelling from left to right. It would appear that the majority of the incident wave energy is reflected back toward the source, and a lesser amount is transmitted through the barrier to be detected at the receiver. To aid visualisation, the simulation domain has been duplicated to give the impression of an array 6 columns wide.

4 Conclusion

In this paper, FDTD simulations were performed in both 3-D and 2-D rectilinear meshes to predict the presence of a

PBG when acoustic waves propagate through an array of cylindrical scatterers 6 rows deep. The objective behind the experiment was to obtain suitable IRs for performing auralizations of sonic crystals, and to compare the results of the 2-D and 3-D simulations.

Results from both sets of simulations show some correspondence between the predicted locations of the band-gaps and their actual locations. The fundamental band-gaps are of most interest, as it is presumed the method of prediction becomes less valid at subsequent band-gaps due to the complexity of the wave interaction and the discrete nature of the model - for example, errors associated with the restricted resolution of the inclusions are cumulative with frequency. Moreover, the basis of our predictions was rudimentary, and in future work we intend to adopt a theoretical approach used in electromagnetics known as the Plane Wave Expansion (PWE) method [12].

As anticipated, the results of the 3-D simulations using the planar source are very similar to those of the 2-D simulations. This is an important result as it confirms that our 3-D model is reliable enough to start investigating more complex triply periodic structures. This will be the main focus of future work, as it is believed that the pronounced filtering effects observed in the 2-D sonic crystals may be even more extreme in the 3-D case. Furthermore, from a purely aesthetic viewpoint, it is believed that 3-D sonic crystals may be less limited in their power to both captivate and stimulate the imagination of an observer.

Acknowledgment

This work is supported by a University of York EPSRC sponsored Doctoral Training Grant.

References

References

- [1] B. Blesser and L.-R. Salter, *Spaces Speak, Are You Listening?* MIT Press, 2007.
- [2] J. S. V. G. J. L. R. Martinez-Sala, J. Sánchez and F. Meseguer, "Sound attenuation by sculpture," *Nature (London)*, vol. 378, p. 241, 1995.
- [3] R. M. R. S. J.V. Sanchez-Perez, C. Rubio and R. Gomez, "Acoustic barriers based on periodic arrays of scatterers," *Applied Physics Letters*, vol. 81, pp. 5240–5242, 2002.
- [4] Liminal, "The organ of corti," jan 2012.
- [5] O. Solon, "Organ of Corti sculpts sound." <http://www.wired.co.uk>, 2011.
- [6] W. Robertson and J. R. III, "Measurement of acoustic stop bands in two-dimensional periodic scattering arrays," *J. Acoust. Soc. Am.*, vol. 104, pp. 694–699, 1998.
- [7] T. Miyashita, "Sonic crystals and sonic waveguides," *IOP Publishing: Meas. Sci. Technol.*, vol. 16, 2005.
- [8] K. Kowalczyk and M. van Walstijn, "Room acoustics simulation using 3-d compact explicit fdtd schemes," *IEEE Transactions on Audio, Speech, and Language Processing*, vol. 19, jan 2011.
- [9] S. Hoare, "Auralization of sonic crystals through simulation of acoustic band gaps in 2-d periodic scattering arrays," in *Proc. of IEEE Workshop on Applications of Signal Processing to Audio and Acoustics*, (New Paltz, NY), oct 2011.
- [10] K. Kowalczyk, *Boundary and medium modelling using compact finite difference schemes in simulations of room acoustics for audio and architectural design applications*. PhD thesis, Queens University Belfast, 2008.
- [11] K. Kunz and R. Luebbers, *The Finite Difference Time Domain Method for Electromagnetics*. CRC Press, 1993.
- [12] S. G. Johnson and J. Joannopoulos, *Introduction to Photonic Crystals: Bloch's Theorem, Band Diagrams, and Gaps (But No Defects)*. MIT, 2003.

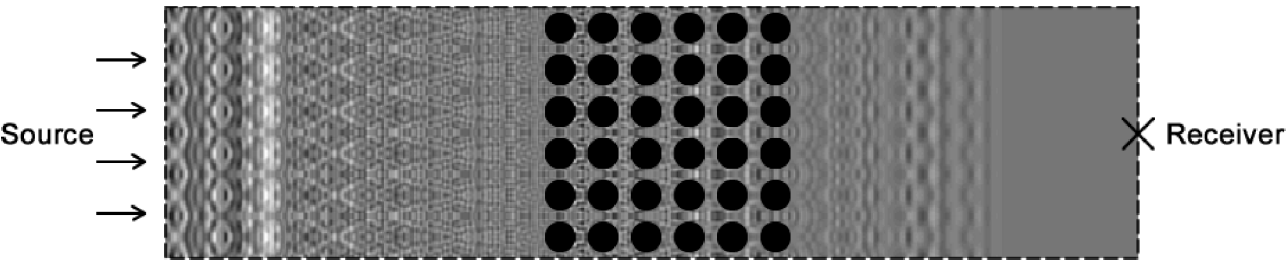


Figure 7: 2-D simulation at $t = 7\text{ms}$.

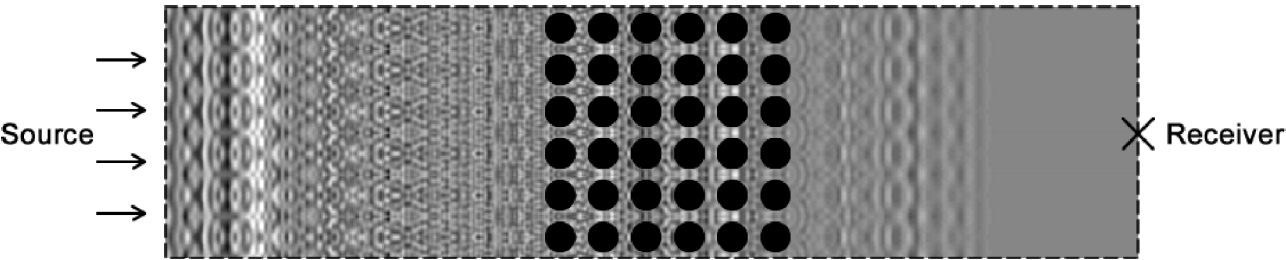


Figure 8: Horizontal slice through 3-D simulation at $t = 7\text{ms}$.

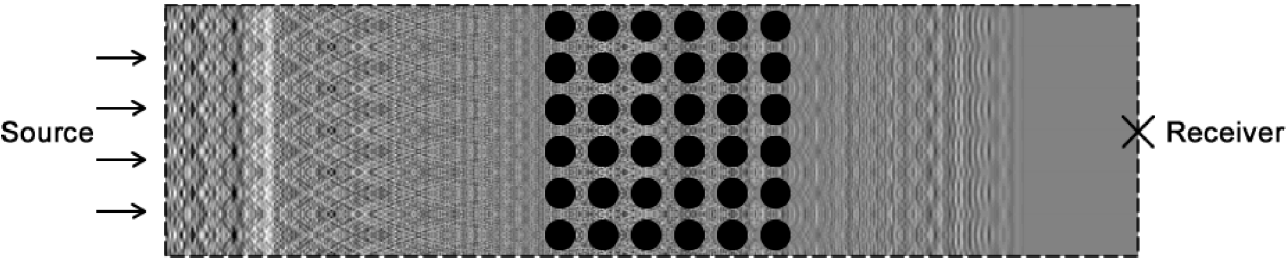


Figure 9: 2-D simulation at $t = 7\text{ms}$.

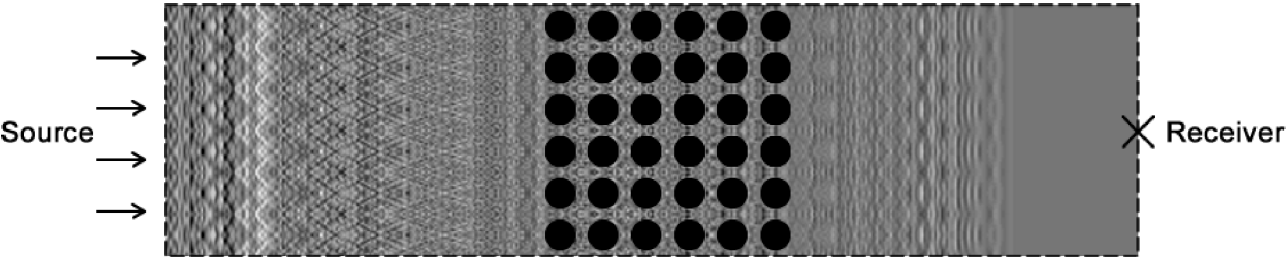


Figure 10: Horizontal slice through 3-D simulation at $t = 7\text{ms}$.

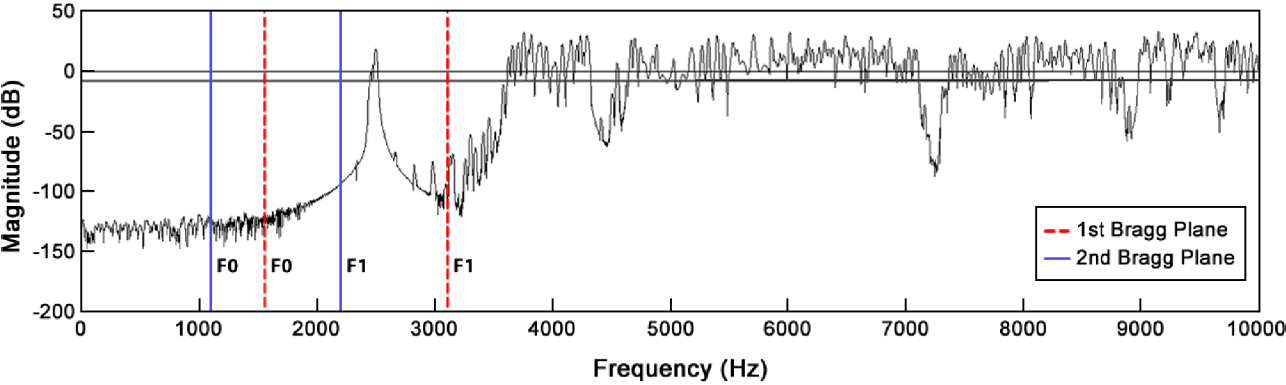


Figure 11: Fast Fourier Transform of the 2-D IR before and after the barrier is inserted compared. $dx = 5\text{mm}$, $F_s = 96.9\text{kHz}$, duration = 115ms.

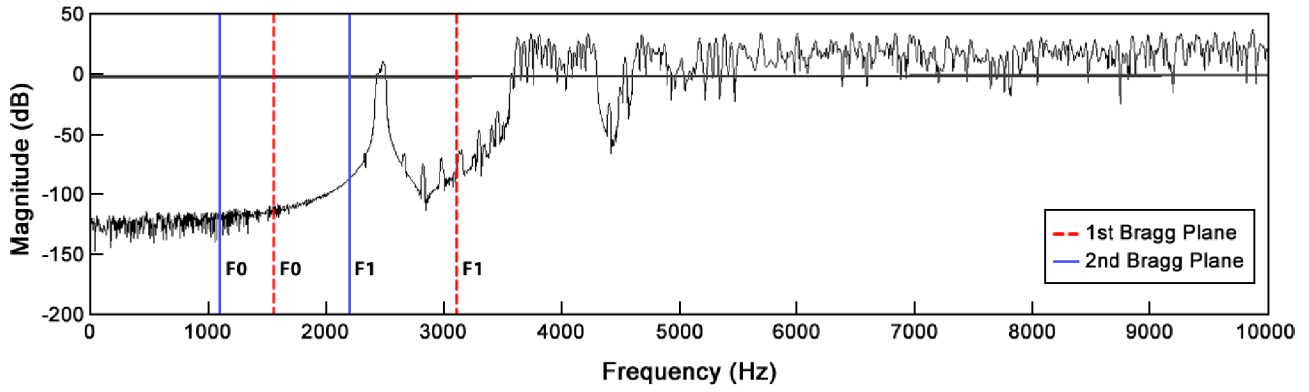


Figure 12: Fast Fourier Transform of the 3-D IR before and after the barrier is inserted. $dx = 5\text{mm}$, $F_s = 118.7\text{kHz}$, duration = 98ms.

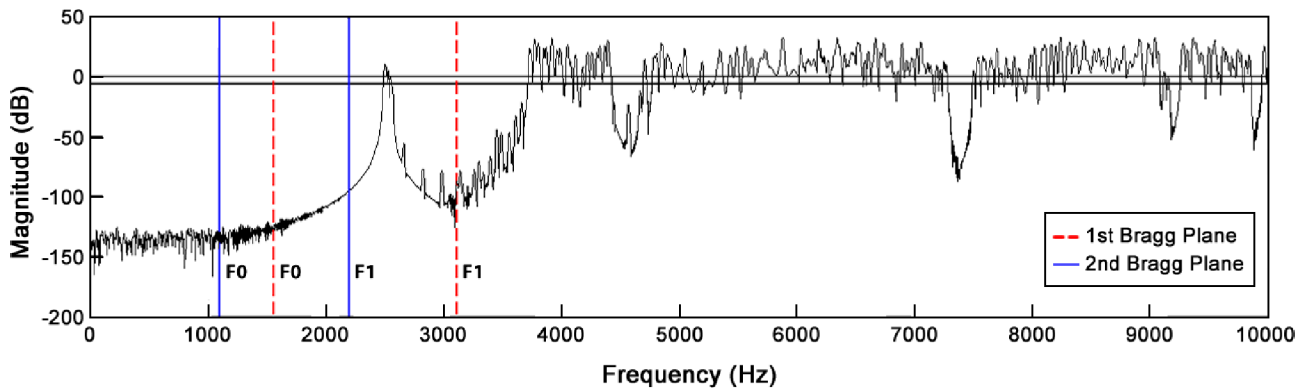


Figure 13: Fast Fourier Transform of the 2-D IR before and after the barrier is inserted compared. $dx = 2.5\text{mm}$, $F_s = 193.8\text{kHz}$, duration = 115ms.

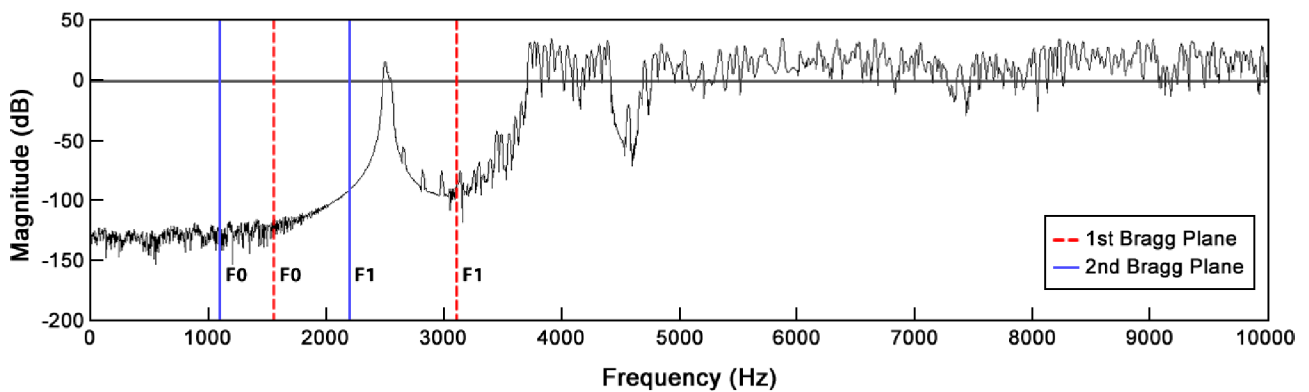


Figure 14: Fast Fourier Transform of the 3-D IR before and after the barrier is inserted. $dx = 2.5\text{mm}$, $F_s = 237.3\text{kHz}$, duration = 98ms.